Distributed Control of Laminated Beams: Timoshenko Theory vs. Euler-Bernoulli Theory

OSAMA J. ALDRAIHEM,* ROBERT C. WETHERHOLD** AND TARUNRAJ SINGH
Department of Mechanical and Aerospace Engineering, State University of New York, Buffalo, NY 14260-4400

ABSTRACT: In this paper, the governing equations and boundary conditions of laminated beam-like components of smart structures are reviewed. Sensor and actuator layers are included in the beam so as to facilitate vibration suppression. Two mathematical models, namely the shear-deformable (Timoshenko) model and the shear-indeformable (Euler-Bernoulli) model, are presented. The differential equations of the continuous system are approximated by utilizing finite element techniques for both models. A cantilever laminated beam with and without a tip mass is investigated to assess the validity and the accuracy of the two models when used for vibration suppression. Comparison between the two models is presented to show the advantages and the limitations of each of the models. Since the Timoshenko beam theory is higher order than the Euler- Bernoulli theory, it is known to be superior in predicting the transient response of the beam. The superiority of the Timoshenko model is more pronounced for beams with a low aspect ratio. It is shown that use of an Euler-Bernoulli based controller to suppress beam vibration can lead to instability caused by the inadvertent excitation of unmodelled modes.

INTRODUCTION

MODELING and control of light flexible structures have become a subject of interest in recent years. One attractive and compact way for vibration control of many space and earth flexible structures is by incorporating into the structure a smart material actuator such as a piezoceramic. Surface mounted or embedded piezoceramic actuators have been reported to successfully suppress undesired structural vibrations [1–3]. Although numerous researchers [4,5] have well established a mathematical shear-indeformable model, modeling of the adaptive structures by shear deformable theory is limited [6].

Shear effects in the distributed control of a laminated beam become important when a high degree of accuracy is crucial, for beams whose length to thickness (aspect) ratio is less than 15 for isotropic materials and less than 30 for composite materials, and where a tip mass is present. Since many smart structures contain composite layer(s) and since an aspect ratio of 30 or less is quite possible, shear effects cannot be ignored. Consequently, a shear-deformable model can be useful for providing more accurate control of vibration.

In this work, detailed shear-deformable (Timoshenko) and shear-indeformable (Euler-Bernoulli) models are established for a laminated beam, and their application to distributed dynamic measurement and active vibration control is investigated. A finite element formulation is presented for both models. Finally, the validity and accuracy of the Euler-Bernoulli model are compared with those of the Timoshenko model by simulating the vibration control of a cantilever laminated beam over various aspect ratios and with and without a tip mass.

*Currently: Department of Mechanical Engineering, King Saud University, P.O. Box 800—Riyadh 11421, Kingdom of Saudi Arabia.
**Author to whom correspondence should be addressed.

EQUATIONS OF MOTION

Displacement Assumptions

Consider a symmetric laminated beam as shown in Figure 1. The laminate is made up of smart laminae, each of which can serve as a sensor/actuator (i.e., PZT, PVF_2), and a host structure. The length, width, and thickness of the beam are denoted by L, b and h, respectively. It is assumed that the beam centroidal and elastic axes coincide with the x axis. Using the usual Timoshenko assumptions, the beam is assumed to undergo deflections with a displacement field of the form

$$u(x,y,z,t) \approx z\phi(x,t) \tag{1a}$$

$$v(x,y,z,t) \approx 0 \tag{1b}$$

$$w(x,y,z,t) \approx W(x,t) \tag{1c}$$

where ϕ is the rotation of the beam cross-section about the positive y axis and W is the transverse displacement of a point on the centroidal axis ($y=z=0$). Note that the axial vibration of the beam centerline is assumed negligible, as is the expansional strain in the axial direction. This can be accomplished, for example, by having actuator layers act in symmetric pairs at equal distance from the beam centerline and with opposite piezoelectric strain.

1045-389X/97/02 0149-09 $10.00/0

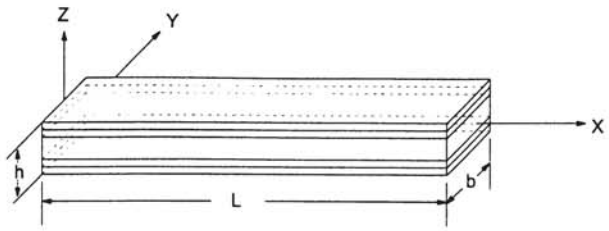

Figure 1. *Laminated beam coordinate system.*

The strain displacement relations can be applied to Equation (1) to give

$$S_x = z\kappa_x, \quad \kappa_x = \frac{\partial \phi}{\partial x} \tag{2a}$$

$$S_{xz} = \phi + \frac{\partial W}{\partial x} \tag{2b}$$

The constitutive equations can be written in the presence of only piezoelectric expansional strains as

$$T_x = Y(S_x - S_x^a) \tag{3a}$$

$$T_{xz} = G_{xz}S_{xz} \tag{3b}$$

with actuation strain

$$S_x^a = d_{31}' E_3 \tag{4}$$

where (Y,G_{xz}) are the appropriate beam (tensile, shear) moduli, d_{31}' is the piezoelectric coupling constant, and E_3 is the electric field applied on the actuator lamina in the z direction.

In Euler-Bernoulli theory, the transverse shear deformation is set to zero, and the displacement field [Equations 1(a)–1(c)] is simplified to

$$u(x,y,z,t) = -z\frac{\partial W}{\partial x} \tag{5a}$$

$$w(x,y,z,t) = W(x,t) \tag{5b}$$

and the strain displacement relations give

$$S_x = z\kappa_x, \quad \kappa_x = -\frac{\partial^2 W}{\partial x^2} \tag{6a}$$

$$S_{xz} = 0 \tag{6b}$$

Hamilton's Principle

The equations of motion along with the boundary conditions of a laminated beam are derived via Hamilton's principle

$$\int_{t_1}^{t_2} \delta(T - V)dt + \int_{t_1}^{t_2} \delta W_{nc}\, dt = 0 \tag{7}$$

where δ is the first variation operator, T is the total kinetic energy of the system (beam, attached masses, etc.) V is the potential (strain) energy, and δW_{nc} is the virtual work done by the nonconservative forces and/or moments (e.g., transverse load or boundary load). If the only expansion-induced moments are piezoelectric and if the structure has no bending-twisting coupling, the δW_{nc} term in Equation (7) is easily formulated as $M^a\delta\kappa_x$, and the usual strain-energy definition can be used. If bending-twisting structural coupling is present through D_{16} or an eccentric tip mass, the definition of W_{nc} may not be obvious. In this case, the strain energy may be redefined to include expansional strain terms including thermal and piezoelectric effects; this eliminates the need for an ad hoc δW_{nc} term.

The equations of motion of a Timoshenko beam are

$$I_1 \frac{\partial^2 W}{\partial t^2} - (GA)^b \left(\frac{\partial^2 W}{\partial x^2} + \frac{\partial \phi}{\partial x}\right) = 0 \tag{8}$$

$$I_3 \frac{\partial^2 \phi}{\partial t^2} - (EI)^b \frac{\partial^2 \phi}{\partial x^2} + (GA)^b \left(\frac{\partial W}{\partial x} + \phi\right) = -\frac{\partial M^a}{\partial x} \tag{9}$$

where

$$(I_1, I_3) = b\int_{-h/2}^{h/2} \rho(1, z^2)dz$$

$$(GA)^b = kb\int_{-h/2}^{h/2} G_{xz}dz, \quad k \approx 5/6$$

$$(EI)^b = b\int_{-h/2}^{h/2} Yz^2 dz$$

$$M^a = b\int_{-h/2}^{h/2} Yd_{31}' E_3 z dz$$

with admissible boundary conditions:

either W prescribed or

$$Q = (GA)^b\left(\phi + \frac{\partial W}{\partial x}\right) + \underline{M_t\left(\frac{\partial^2 W}{\partial t^2} - c\frac{\partial^2 \phi}{\partial t^2}\right)} \text{ prescribed} \tag{10a}$$

and either ϕ prescribed or

$$-M = M^a - (EI)^b \frac{\partial \phi}{\partial x} + \underline{M_t\left(\frac{\partial^2 W}{\partial t^2} - c\frac{\partial^2 \phi}{\partial t^2}\right)\cdot c - I_o \frac{\partial^2 \phi}{\partial t^2}} \text{ prescribed} \tag{10b}$$

where

$$M = b\int_{-h/2}^{h/2} T_x z dz$$

$$Q = b\int_{-h/2}^{h/2} T_{xz} dz$$

The underlined terms exist only when there is a spherical tip mass M_t of radius c at the free end of the beam; the effect of the rotatory inertia I_o of the tip mass about the y-axis is included. The equation of motion of a laminated Euler-Bernoulli beam is

$$I_1 \frac{\partial^2 W}{\partial t^2} + (EI)^b \frac{\partial^4 W}{\partial x^4} = -\frac{\partial^2 M^a}{\partial x^2} \tag{11}$$

with the admissible boundary conditions:

either $\partial W/\partial x$ prescribed or

$$-M = (EI)^b \frac{\partial^2 W}{\partial x^2} + M^a + \underline{M_t \cdot c\left(\frac{\partial^2 W}{\partial t^2} + c\frac{\partial^3 W}{\partial x \partial t^2}\right) + I_o \frac{\partial^3 W}{\partial x \partial t^2}} \text{ prescribed} \tag{12a}$$

and either W prescribed or

$$-Q = (EI)^b \frac{\partial^3 W}{\partial x^3} + \frac{\partial M^a}{\partial x} - \underline{M_t\left(\frac{\partial^2 W}{\partial t^2} + c\frac{\partial^3 W}{\partial x \partial t^2}\right)} \text{ prescribed} \tag{12b}$$

where Q is the shear force; $Q = dM/dx$.

The underlined terms exist only when there is a tip mass; the rotatory inertia of the tip mass is included.

SENSOR EQUATION

In this section, we will develop the sensor equation of a spatially distributed piezoelectric lamina for both Euler-Bernoulli and Timoshenko beam models. Either a series of distributed sensor patches or a continuous patch which covers the entire beam can detect all modes of vibration [7]. Furthermore, the sensor layer can be a separate layer, as in our illustration case, or it can be the actuator layer itself [8]. The sensor equation relates the in-plane beam displacements and curvatures to the output charge signal which may be used for feedback to the piezoactuator layers. When the laminated beam is deformed, an electric displacement is generated on the sensor lamina.

$$D_3 = Y_s d'_{31} S_x \tag{13}$$

where Y_s is the sensor Young's modulus, d'_{31} is the sensor piezoelectric constant, and S_x is the beam normal strain given in Equation (6a) for the Euler-Bernoulli beam and given in Equation (2a) for the Timoshenko beam.

Employing Gauss' law [3] and Equations 2(a), 6(a) and (13), and assuming that the effective surface electrode of the sensor is uniform and equal to the in-plane area of the beam, the charge enclosed by the sensor electrodes is approximated by

$$q^k(t) = -b\int_0^L d'_{31} Y_s \bar{z}_k \left(\frac{\partial^2 W}{\partial x^2}\right) dx \tag{14a}$$

Euler-Bernoulli charge sensor

$$q^k(t) = b\int_0^L d'_{31} Y_s \bar{z}_k \left(\frac{\partial \phi}{\partial x}\right) dx \tag{14b}$$

Timoshenko charge sensor

where $\bar{z}_k$ is the signed distance from the beam centroid to the centroid of sensor layer k. It may be possible to differentially pole the sensor over its surface area so that the coupling coefficient $d'_{31} = d'_{31}(x) = d^o_{31} f(x)$ in order to sense certain vibration modes [7], where d^o_{31} is a nominal or average value. For this paper, it is assumed that d'_{31} is constant and equal to d^o_{31}. Owing to the fact that the electric charge is difficult to measure directly, the voltage form of the sensor equation is necessary for modeling a measurable quantity. This is achieved by multiplying Equations 14(a) and 14(b) by the reciprocal of the sensor capacitance C_s:

$$V^k(t) = \frac{-bY_s \bar{z}_k}{C_s}\int_0^L d'_{31} \frac{\partial^2 W}{\partial x^2} dx$$

Euler-Bernoulli voltage sensor (15a)

$$V^k(t) = \frac{-bY_s \bar{z}_k}{C_s}\int_0^L d'_{31} \frac{\partial \phi}{\partial x} dx$$

Timoshenko voltage sensor (15b)

The very useful (current) form of the sensor equation for the design of active control systems is achieved by taking the time derivative of the charge equation (14).

$$i^k(t) = -bY_s\bar{z}_k\int_0^L d'_{31}\frac{\partial^3 W}{\partial t\partial x^2}\,dx$$

Euler-Bernoulli current sensor (16a)

$$i^k(t) = bY_s\bar{z}_k\int_0^L d'_{31}\frac{\partial^2 \phi}{\partial t\partial x}\,dx$$

Timoshenko current sensor (16b)

If the sensor properties are constant in the spatial variable x, then the integrals found in Equations (14) through (16) can be evaluated in terms of values at the endpoints ($x = 0,L$).

A close examination of all the forms of the sensor equations shows that the voltage form [Equation (15)] is appropriate for displacement measurement while the current form [Equation (16)] is suitable for velocity measurement at any point on the flexible beam. Furthermore, the conventional piezoelectric sensor can only detect bending deformation (normal strain). If we are trying to control the deflection at the end of the beam $W(L)$, this can create difficulty for a "short" beam where shear deformation is comparable to bending deformation. The sensor signal is sensitive to only part of the deformation, and we can expect a longer settling time after a disturbance.

LYAPUNOV BASED CONTROL LAW

Flexible beam-like structures are distributed-parameter systems having an infinite number of modes. It is a common procedure to model the system with a finite number of modes and design a control system using lumped parameter control theory. Truncating the model may lead to performance degradation when designing a control system for the distributed parameter system. Consequently, we shall derive a controller for vibration suppression of a laminated beam without discretization. Piezoceramic layers symmetrically and perfectly bonded to the flexible beam are used to perform the actuation. The control law is established based on the Lyapunov second or direct method. In this method, one proposes a positive definite Lyapunov functional of the system and chooses the control law to guarantee that the time derivative of the functional is negative semi-definite or negative definite. A basic candidate functional is the energy (kinetic and potential) in the system.

$$F = \frac{1}{2}\int_0^L\left[I_1\left(\frac{\partial W}{\partial t}\right)^2 + (EI)^b\left(\frac{\partial^2 W}{\partial x^2}\right)^2\right]dx$$

$$\underline{+\frac{1}{2}M_t\left(\left.\frac{\partial W}{\partial t}\right|_{x=L} + c\left.\frac{\partial^2 W}{\partial t\partial x}\right|_{x=L}\right)^2}$$

$$\underline{+\frac{1}{2}I_o\left(\left.\frac{\partial^2 W}{\partial t\partial x}\right|_{x=L}\right)^2}, \text{ Euler-Bernoulli} \quad (17a)$$

$$F = \frac{1}{2}\int_0^L\left[I_1\left(\frac{\partial W}{\partial t}\right)^2 + I_3\left(\frac{\partial \phi}{\partial t}\right)^2 + (EI)^b\left(\frac{\partial \phi}{\partial x}\right)^2 + (GA)^b\left(\phi^2 + 2\phi\frac{\partial W}{\partial x} + \left(\frac{\partial W}{\partial x}\right)^2\right)\right]dx$$

$$\underline{+\frac{1}{2}M_t\left(\left.\frac{\partial W}{\partial t}\right|_{x=L} - c\left.\frac{\partial \phi}{\partial t}\right|_{x=L}\right)^2}$$

$$\underline{+\frac{1}{2}I_o\left(\left.\frac{\partial \phi}{\partial t}\right|_{x=L}\right)^2}, \text{ Timoshenko} \quad (17b)$$

The underlined terms are present only when there is a tip mass. Differentiating the Lyapunov functional [Equation (17)] with respect to time, employing the differential Equations (8), (9) and (11), and using boundary conditions for a cantilever beam fixed at $x = 0$ and free at $x = L$ yields

$$\frac{dF}{dt} = \int_0^L -\frac{d^2M^a}{dx^2}\left(\frac{\partial W}{\partial t}\right)dx - M^a\left(\frac{\partial^2 W}{\partial t\partial x}\right)_{x=L} + \frac{dM^a}{dx}\left(\frac{\partial W}{\partial t}\right)_{x=L}, \text{ Euler-Bernoulli} \quad (18a)$$

$$\frac{dF}{dt} = \int_0^L \frac{dM^a}{dx}\left(\frac{\partial \phi}{\partial t}\right)dx + M^a\left(\frac{\partial \phi}{\partial t}\right)_{x=L}, \text{ Timoshenko} \quad (18b)$$

For any other boundary conditions, the time derivative of the proposed Lyapunov functional can be derived by following the same procedure.

In practice, the actuators are likely to cover part of the beam surface. For simplicity of illustration, we assume that the piezoelectric actuators are uniform and completely cover the transverse faces of the host beam. Thus, the actuation moment M^a is only a function of time with all of its spatial derivatives being identically zero. Equation (18) thus becomes

$$\frac{dF}{dt} = -M^a\left(\frac{\partial^2 W}{\partial t\partial x}\right)_{x=L}, \text{ Euler-Bernoulli} \quad (19a)$$

$$\frac{dF}{dt} = M^a\left(\frac{\partial \phi}{\partial t}\right)_{x=L}, \text{ Timoshenko} \tag{19b}$$

Consider a pair of actuator layers with a common ground and identical poling directions. Through differentially poling over the actuator surface, it is possible to produce an actuator whose d'_{31} varies spatially and which controls certain modes [7]. For this paper, it is assumed that d'_{31} is constant. The actuation moment in Equation (19) can be written in terms of actuator input voltage as follows

$$M^a = J_1 V_a(t) \tag{20}$$

with

$$J_1 = 2bY_a d'_{31}\bar{z}_a$$

where Y_a and $\bar{z}_a$ are the actuator Young's modulus and (positive) distance from the centerline, respectively. The time derivative of the Lyapunov functional is negative semidefinite if and only if the actuator voltage is selected as

$$V(t) = +G_1 J_1\left(\frac{\partial^2 W}{\partial t \partial x}\right)_{x=L}, \text{ Euler-Bernoulli} \tag{21a}$$

$$V(t) = -G_2 J_1\left(\frac{\partial \phi}{\partial t}\right)_{x=L}, \text{ Timoshenko} \tag{21b}$$

where G_1 and G_2 are positive gain constants.

It should be noted that the time derivative of the Lyapunov functional [Equation (19)] for both models is negative semidefinite, implying stability only. Nevertheless, asymptotic stability has been proven in a recent paper [9] using the theorem given by Mukherjee and Chen [10].

FINITE ELEMENT FORMULATION

Consider a beam element of length h_e which has two degrees of freedom at each node: one translational degree of freedom and one rotational degree of freedom (Figure 2). The beam element's transverse deflection and the beam element rotation angle are approximated by [11]

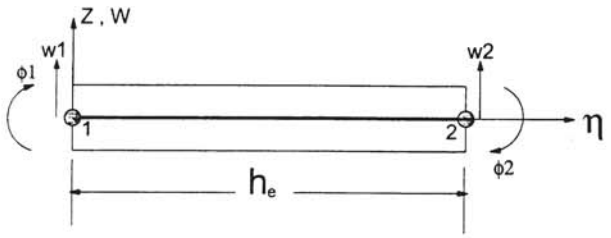

Figure 2. *Beam element.*

$$W(x,t) = \sum_{i=1}^{4} N_i^w(x)\Delta_i(t) \tag{22a}$$

$$\phi(x,t) = \sum_{i=1}^{4} N_i^\phi(x)\Delta_i(t) \tag{22b}$$

where Δ_i are the nodal displacements and rotations given as

$$\Delta = \begin{Bmatrix} W_1 \\ \phi_1 \\ W_2 \\ \phi_2 \end{Bmatrix} \tag{23}$$

and (N_i^w, N_i^ϕ) are the shear-locking-free shape functions which are assumed to have the following form (Equation [11], with some sign corrections)

$$N^w = \begin{bmatrix} \frac{1}{1+\nu}(2\zeta^3 - 3\zeta^2 - \nu\zeta + 1 + \nu) \\ \frac{-h_e}{1+\nu}\left(\zeta^3 - \left(2+\frac{\nu}{2}\right)\zeta^2 + \left(1+\frac{\nu}{2}\right)\zeta\right) \\ \frac{-1}{1+\nu}(2\zeta^2 - 3\zeta^2 - \nu\zeta) \\ \frac{-h_e}{1+\nu}\left(\zeta^3 - \left(1-\frac{\nu}{2}\right)\zeta^2 - \frac{\nu}{2}\zeta\right) \end{bmatrix} \tag{24a}$$

$$N^\phi = \begin{bmatrix} \frac{-6}{(1+\nu)h_e}(\zeta^2 - \zeta) \\ \frac{1}{1+\nu}(3\zeta^2 - (4+\nu)\zeta + 1 + \nu) \\ \frac{6}{(1+\nu)h_e}(\zeta^2 - \zeta) \\ \frac{1}{1+\nu}(3\zeta^2 - (2-\nu)\zeta) \end{bmatrix} \tag{24b}$$

with the rigidity ratio [$\nu = 12(EI)^b/h_e^2(GA)^b$ for Timoshenko model; $\nu = 0$ for Euler-Bernoulli model] and the dimensionless quantity $\zeta = \eta/h_e$, where η is the element local coordinate [Figure (2)].

For n finite elements the discrete differential equations of the laminated beam are obtained by using Equation (22) to evaluate the kinetic energy and strain energy of the beam. Integrating over the spatial domains and using Hamilton's principle (7) leads to

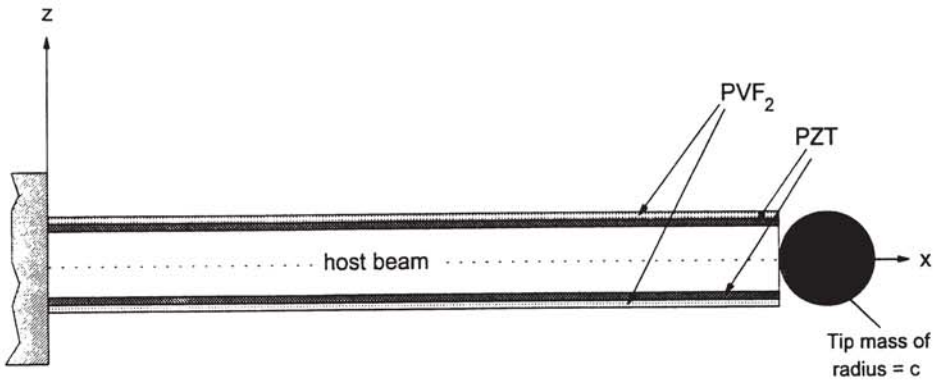

Figure 3. *Laminated beam configuration.*

$$[M]_{(2n\times 2n)}\left\{\frac{d^2\Delta}{dt^2}\right\}_{(2n\times 1)} + [K]_{(2n\times 2n)}\left\{\frac{d\Delta}{dt}\right\}_{(2n\times 1)} = \{D\}_{(2n\times 1)}u(t)_{(1\times 1)} \tag{25}$$

where $u(t)$ is the input to the system and $[M]$, $[K]$ and $\{D\}$ are the global mass, stiffness, and control influence matrices, respectively, which are given as

$$[M] = \int_0^L \left[\{N^w\}\{N^\phi\}\right]_{(4\times 2)} \times \begin{bmatrix} I_1 & 0 \\ 0 & I_3 \end{bmatrix}_{(2\times 2)} \begin{bmatrix} \{N^w\}^T \\ \{N^\phi\}^T \end{bmatrix}_{(4\times 2)} dx, \text{ Timoshenko} \tag{26a}$$

$$[M] = \int_0^L \{N^w\}(I_1)\{N^w\}^T dx, \text{ Euler-Bernoulli} \tag{26b}$$

$$[K] = \int_0^L \begin{bmatrix} \frac{d}{dx}\{N^\phi\}^T \\ \{N^\phi\}^T + \frac{d}{dx}\{N^w\}^T \end{bmatrix}^T \begin{bmatrix} (EI)^b & 0 \\ 0 & (GA)^b \end{bmatrix} \times \begin{bmatrix} \frac{d}{dx}\{N^\phi\}^T \\ \{N^\phi\}^T + \frac{d}{dx}\{N^w\}^T \end{bmatrix} dx, \text{ Timoshenko} \tag{27a}$$

$$[K] = \int_0^L \left\{\frac{d}{dx}N^\phi\right\}(EI)^b\left\{\frac{d}{dx}N^\phi\right\}^T dx, \text{ Euler-Bernoulli} \tag{27b}$$

$$\{D\} = \int_0^L \left\{\frac{d}{dx}N^\phi\right\} dx, \text{ for both models} \tag{28}$$

Equation (25) can easily be generalized to allow for p multiple, independent control voltages; $\{D\}$ will become $(2n \times p)$ and $u(t)$ will become $(p \times 1)$.

It should be noted that the rotational degree of freedom for the Euler-Bernoulli model is the negative of the beam slope: $\phi = -\partial W/\partial x$. We could reformulate the finite element representation of the Euler-Bernoulli model to take advantage of the fewer degrees of freedom. Instead, we choose to simplify the representation internally. The second and fourth elements of the shape functions of Equations (24a) and (24b) should be multiplied by negative one to enforce the condition $\phi = -\partial w/\partial x$. This in turn causes the second and fourth column and row of the element mass and stiffness matrices of the Euler-Bernoulli model to change sign. This will permit the interchange of information between the two models when investigating their relative efficiency.

NUMERICAL SIMULATION

In this section, we consider a five layer cantilever laminate with stacking sequence: PVF_2, PZT, Al, PZT, PVF_2. A sketch of this laminated beam configuration is shown in Figure 3. The piezopolymer layers function as distributed sensors, whereas the piezoceramic layers perform the actuation. The top and bottom piezoelectric (sensor/actuator) layers are positioned with identical poling directions for effective sensing and strong actuation. The effectiveness of these types of active beam elements in suppressing the vibration of a laminated beam is investigated below for both Timoshenko and Euler-Bernoulli models and an efficiency comparison is demonstrated.

Table 1. Material properties.

	Y (GPa)	G_{xz} (GPa)	d'_{31} 10^{-12} (m/V)	ρ (kg/m^3)
PVF_2 [12]	2.0	0.77	23	1780
PZT [13]	81.3	25.65	−123	7500
Al [14]	73	29.2	—	2840

Numerical simulations have been performed for two groups of laminated beams. In the first group, the beams have a tip mass; in the second group, the beams are without tip mass. The behavior of both groups with respect to aspect ratio is illustrated. The beam material properties are listed in Table 1. A finite element code which calculates the matrices established in the preceding section has been developed for calculating the beam transient response. In all simulation cases, the total beam thickness was fixed and the beam length was varied to change the aspect ratio. The sensor and actuator layers were assumed to have thicknesses of 0.11 (mm) and 0.5 (mm), respectively. The host aluminum beam has a thickness five times that of the actuator layer and the width of all layers is twice the total beam thickness. Furthermore, the beam is subdivided into 10 equal-length elements along its length and subjected to displacement initial conditions equivalent to those which would be generated by a tip transverse load that produces a tip deflection equal to 5% of the beam length. The initial beam velocity is zero. The controller gains (G_1, G_2) of both models are selected such that the maximum voltage applied to the actuator layers does not exceed 500 V. This is physically realistic, and is representative of typical power supplies. For the cases in which a tip mass exists, a spherical aluminum tip mass with radius $c = h/4$ was assumed.

All simulation cases for all aspect ratios with and without a tip mass illustrate the asymptotic stability of both beam models. This is expected because the controller designs were based on the Lyapunov second method, and were independent of the beam aspect ratio or presence of a tip mass. As a first basis of comparison of the two beam models, the two percent settling time of the Euler-Bernoulli beam is compared to that of the Timoshenko beam. Figure 4 shows an interesting result of the Euler-Bernoulli model settling time normalized by the Timoshenko model settling time for various values of aspect ratio (L/h). The trends in Figure 4 can be explained clearly with the aid of the beam energies. Because the shear strain energy is neglected in the Euler-Bernoulli model, its strain energy is always calculated to be less than that of the Timoshenko beam. The energies of the two models approach the same value for long beams. Although the rotatory inertia contributes to the kinetic energy of the Timoshenko beam, for short beams the kinetic energy of the Euler-Bernoulli beam is higher. This is because the Euler-Bernoulli beam vibrates at a higher natural frequency than that of the Timoshenko beam, and we set the initial displacement of both models to be the same. For small aspect ratio, the difference in the kinetic energy between the two beam models is greater than the difference in the strain energy; hence, more time is needed to dissipate the total energy of the Euler- Bernoulli beam. Furthermore, the difference in the kinetic energy between the two beam models reduces more rapidly than the difference in the strain energy with the increase of L/h, causing underestimation of the settling time. The Euler-Bernoulli settling time reaches that of the Timoshenko with further increase in L/h (for long beams). The existence of the tip mass accentuates the difference in the kinetic energy between the two beam models, which makes the settling time curve shift up and to the right from that of the no tip mass case (Figure 4).

To obtain another comparison, we investigate the stability

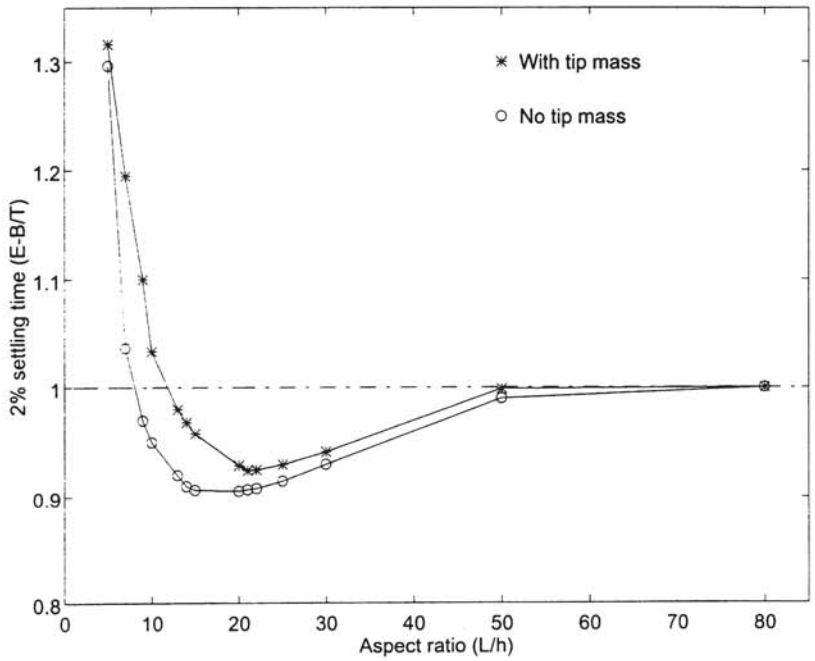

Figure 4. *Two-percent settling time of the Euler-Bernoulli beam normalized by the settling time of the Timoshenko beam.*

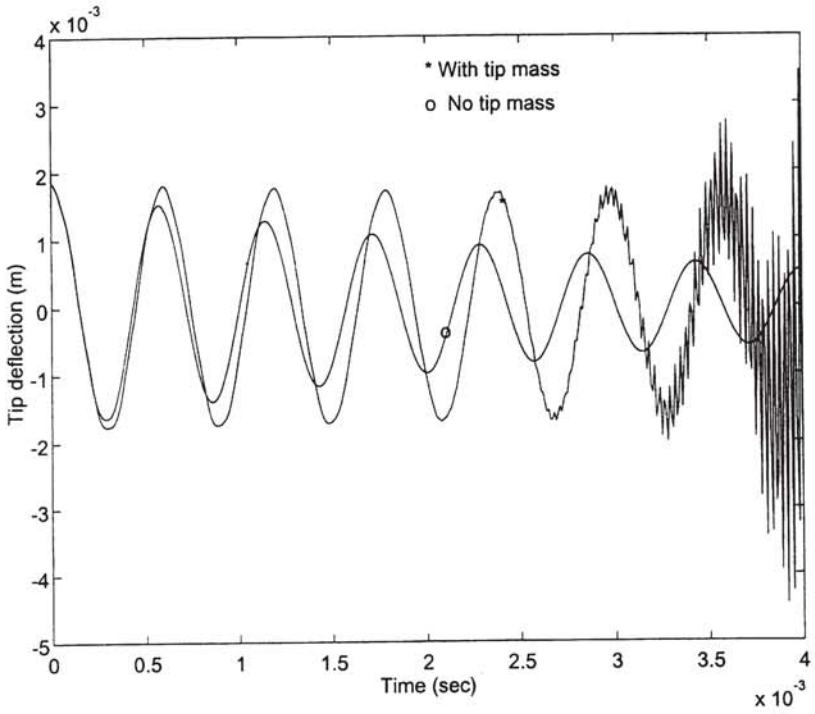

Figure 5. *Timoshenko beam (*L/h = *10) controlled by Euler-Bernoulli controller.*

behavior of a Timoshenko beam of aspect ratio = 10 controlled by an Euler-Bernoulli controller. For this case, the feedback quantity is considered as the negative of the rate of the Timoshenko beam slope instead of the rotation angle rate [set $\phi = -\partial w/\partial x$ in Equation (21b)]. Figure 5 shows that an Euler-Bernoulli model controller can stabilize the cantilever Timoshenko beam when there is no tip mass and will destabilize the beam when there is a tip mass. A careful inspection of the boundary condition [Equation (10a)] when there is no boundary shear force indicates that the Euler-Bernoulli based controller is identical to the Timoshenko controller when there is no tip mass, and is different with the presence of a tip mass. The instability we saw is due to the incorrect assumptions of the Euler-Bernoulli model controller under certain conditions (e.g., short beam and tip mass). It is not that higher order Euler-Bernoulli modes are missing, but rather that certain types of vibration are not being modelled. The significant contribution of shear strain energy to the system dynamics have been ignored in the Euler-Bernoulli modelling and our Euler-Bernoulli controller inadvertently excites these modes. An analogy for this incorrect modelling is the following: we wish to control the axial motion of a bar with a mass on its end by using an axial actuator. Unbeknownst to us, the mass is not on the bar centerline, and torsional and bending vibration of the bar are also present. These additional motions of the bar are not modelled. To the extent that the axial actuator can unwittingly excite torsion and bending motion through the (unmodelled) mass coupling, then instability can result.

CONCLUSIONS

The equations of motion (including actuation) and the sensor equations are established for a Timoshenko beam and for an Euler-Bernoulli beam. These two beam models are investigated and compared by using them to actively control the simulated vibration of beams with and without tip mass and having different aspect ratio. It is shown that the piezoelectric actuator is capable of vibration suppression in beams which have both normal strain as well as shear deformation. The Timoshenko model is clearly superior for beams with low aspect ratio with or without a tip mass. As the aspect ratio of the beam increases, the results of the two models coverage. It has been shown that modeling a beam of low aspect ratio with a tip mass as an Euler-Bernoulli beam can lead to instability of control.

REFERENCES

1. Agrawal, B. N. and H. Bang. 1993. "Active Vibration Control of Flexible Space Structures by Using Piezoelectric Sensors and Actuators", *ASME Vibration and Control of Mechanical Systems,* 61:169–179.
2. Choi, S., C. Cheong and S. Kim. 1995. "Control of Flexible Structures by Distributed Piezofilm Actuators and Sensors", *Journal of Intelligent Materials Systems and Structures,* 6:430–435.
3. Lee, C. K. 1990. "Theory of Laminated Piezoelectric Plates for the Design of Distributed Sensors/Actuators, Part I: Governing Equations and Reciprocal Relationships", *J. Acoust. Soc. Am.,* 87:1144–1158.
4. Bailey, T. and J. E. Hubbard, Jr. 1985. "Distributed Piezoelectric-Polymer Active Vibration Control of a Cantilever Beam", *AIAA Journal of Guidance and Control,* 8:605–611.

5. E. F. Crawley and E. H. Anderson. 1990. "Detailed Models of Piezoelectric Actuation of Beams", *Journal of Intelligent Materials Systems and Structures,* 1:4–25.
6. Zhuang, Y. and J. S. Baras. 1993. "Distributed Control of a Timoshenko Beam", *Proceedings of International Conference on Adaptive Structures* (San Diego, CA), Soc. Photo-Opt Instr., Bellingham, WA, pp. 216–227, Nov. 9–11.
7. Lee, C. K. 1987. "Piezoelectric Laminates for Torsional and Bending Modal Control: Theory and Experiment", Ph.D. dissertation, Cornell University.
8. Dosch, J. J., D. J. Inman and E. Garcia. 1992. "A Self-Sensing Piezoelectric Actuator for Collocated Control", *Journal of Intelligent Materials Systems and Structures,* 3:166–185.
9. Aldraihem, O. J., R. C. Wetherhold and T. Singh. 1996. "Intelligent Beam Structures: Timoshenko Theory vs. Euler-Bernoulli Theory", *Proceedings of the 1996 IEEE International Conference on Control Applications,* Dearborn, MI, pp. 976–981.
10. Mukherjee, R. and D. Chen. 1993. "An Asymptotic Stability Theorem for Autonomous System," *J. Guidance, Control, Dynamics,* 16:960–962.
11. Friedman, Z. and J. B. Kosmatka. 1993. "An Improved Two-Node Timoshenko Beam Finite Element", *Computer and Structures,* 47: 473–481.
12. AMP Piezofilm Sensors. 1993. "Piezoelectric Film-Characteristics", AMP Inc., P. O. Box 799, Valley Forge, PA 19482.
13. Electro Ceramic Division. "Data for Designers", Morgan Matroc Inc., 232 Forbes Road, Bedford, OH 44146.
14. Wetherhold, R. C. and N. Panthalingal. 1994. "Piezoelectric PZT/Epoxy Composites for Controlling Torsional Motion," *J. Intell. Mater. Sys. Struct.,* 5:576–580.
15. Huang, T. C. 1961. "The Effect of Rotary Inertia and of Shear Deformation on the Frequency and Normal Mode Equations of Uniform Beams with Simple End Conditions", *Journal of Applied Mechanics,* 28:579–584.
16. Shieh, R. C. 1993. "Multiaxial Piezoelectric Beam Sensors/Actuators Theory and Design for 3-D Structural Vibration Control", *Proceeding of Third International Conference on Adaptive Structures* (San Diego, CA), Soc. Photo-Opt Instr., Nov. 9-11, Bellingham, WA, pp. 647–661.
17. R. C. Shieh. 1994. "Governing Equations and Finite Element Models for Multiaxial Piezoelectric Beam Sensors/Actuators", *AIAA Journal,* 32:1250–1258.